THE JOURNAL OF PROSTHETIC DENTISTRY

RESEARCH AND EDUCATION

Effects of implant diameter, implant-abutment connection type, and bone density on the biomechanical stability of implant components and bone: A finite element analysis study

Hyeonjong Lee, DMD, PhD,[a] Minhye Jo, BS,[b] Irena Sailer, DMD, PhD,[c] and Gunwoo Noh, PhD[d]

ABSTRACT

Statement of problem. Various kinds of implants of different diameters and connection types are used for patients with a range of bone densities and tooth sizes. However, comprehensive studies simultaneously analyzing the biomechanical effects of different diameters, connection types, and bone densities are scarce.

Purpose. The purpose of this 3-dimensional finite element analysis study was to evaluate the stress and strain distribution on implants, abutments, and surrounding bones depending on different diameters, connection types, and bone densities.

Material and methods. Twelve 3-dimensional models of the implant, restoration, and surrounding bone were simulated in the mandibular first molar region, including 2 bone densities (low, high), 2 implant-abutment connection types (internal tissue level, internal bone level), and 3 implant diameters (3.5 mm, 4.0 mm, and 4.5 mm). The occlusal force was 200 N axially and 100 N obliquely. Statistical analysis was performed using the general linear model univariate procedure with partial eta squared (η_p^2) (α=.05).

Results. For bone tissue, low-density bone induced a larger maximum and minimum principal strain (in magnitude) than high-density bone (P<.001). As the implant diameter increased, the volume of the cancellous bone in low-density bone at the atrophy region (strain<200 $\mu\varepsilon$) increased (P<.001). For implant and abutment, the internal bone-level connection type was associated with increased peak stress as compared with the tissue-level connection type (P<.001). For all models, the stress distribution on the implant complex was influenced by implant diameter (P<.001): a decrease in implant diameter increased the stress concentration.

Conclusions. The implant connection type had a greater impact on the stress of the implant and abutment than the diameter. A tissue-level connection was more advantageous than a bone-level connection in terms of stress distribution of the implant and abutment. Bone density was the most influential factor on bone strain. The selection of dental implants should be made considering these factors and other important factors including tooth size. (J Prosthet Dent 2022;128:716-28)

Various kinds of dental implants of different diameters, lengths, and connection types are currently used in clinical practice, and the long-term success rate of implant-supported restorations has been reported to be 94%.[1,2] However, mechanical complications and failures remain critical issues.[3-6]

A correlation between bone density and strength has been reported,[7] and the different types of implant connection have been analyzed biomechanically.[8-11] The stress distribution of different implant crown heights has been demonstrated; when the crown height is increased, the stress level becomes greater because of the lever effect.[6] Finite element studies of implants have been performed for different factors with various methods,[12-17] including biomechanical analyses of implants as per their diameters, bone densities, and connections. However, the authors are unaware of a study that considered all

Supported by the Basic Science Research Program (Grant No. 2018R1D1A1B07049789) through the National Research Foundation of Korea (NRF) funded by the Ministry of Education.
[a]Assistant Professor, Department of Prosthodontics, Dental Research Institute, Dental and Life Science Institute, School of Dentistry, Pusan National University, Yangsan, Republic of Korea.
[b]Graduate student, School of Mechanical Engineering, Korea University, Seoul, Republic of Korea.
[c]Professor, Division of Fixed Prosthodontics and Biomaterials, Clinique of Universitaire Medicine Dentaire, University of Geneva, Geneva, Switzerland.
[d]Assistant Professor, School of Mechanical Engineering, Korea University, Seoul, Republic of Korea.

Clinical Implications

In patients with low-density cancellous bone, a tissue-level connection should be preferred over an internal bone-level connection because it is associated with better implant and abutment stress distribution and reduced bone strain. If an internal bone-level connection is used for low-density bone, an implant with a diameter of 4.5 mm or greater should be considered.

of these factors simultaneously.[12,13,18] The correlation between the stress and strain analysis of implants and the surrounding structures as per bone density, implant diameter, load of direction, and type of connection in a single controlled study is necessary. Understanding the stress transmission from the implant crown to the implant component and the surrounding bone would be useful for clinicians who must decide on the diameter and connection of the implant based on factors such as the status of residual bone, antagonist, and prosthetic planning.

Several important factors should be considered in the analysis of stress and strain distributions. Strain analysis has been performed on the bone surrounding the implant,[14,15,19-21] and the maximum or minimum strain values at a specific point have been evaluated. As per the mechanostat theory,[22,23] strain values may be classified into 4 regions: atrophy (<200 με), maintenance (200 to 2500 με), hypertrophy (2500 to 4000 με), and fatigue failure (>4000 με). Volumetric analysis of strain as per the mechanostat theory focused around implants could provide more meaningful information than common strain analysis.[24]

To decrease the failure rate of the implant, it is clinically important when selecting an implant to consider various biomechanical factors simultaneously, including bone density, type of connection, diameter, and loading condition, as well as other important factors such as emergence profile, soft-tissue condition, implant position, and esthetics.[25-30] The biotype of the peri-implant soft tissue is also an important variable.[31,32] The purpose of the present finite element analysis study was to analyze the strain distribution of peri-implant hard tissue and stress distribution of implant components for various bone densities, implant diameters, and implant-abutment connection types. The null hypothesis was that different implant diameters, implant-abutment connection types, or bone densities would not result in different stress values in the implant components or different strain values in the surrounding bone near the prosthesis.

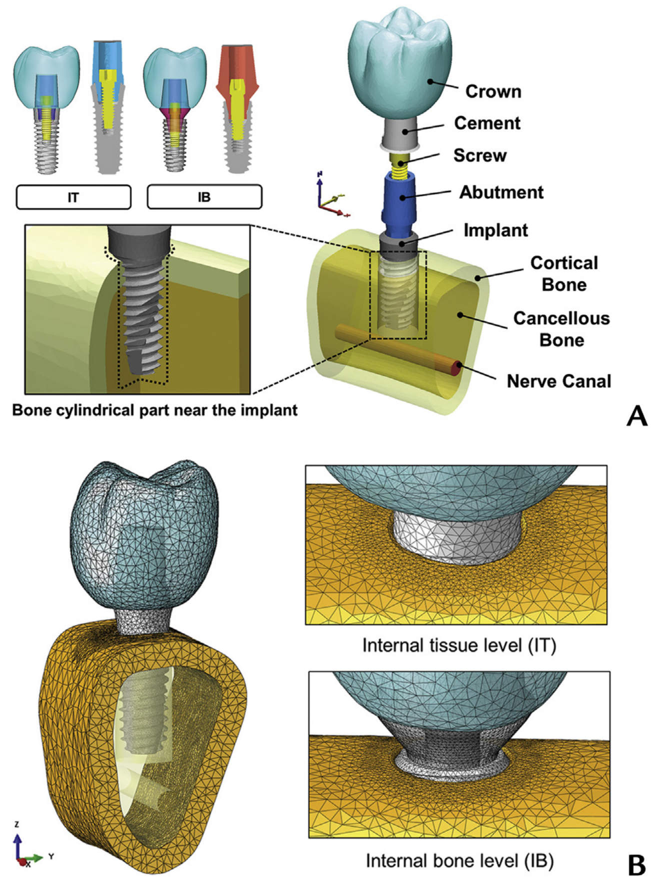

Figure 1. Three-dimensional finite element models and 2 types of implant system. A, Internal tissue level (IT) and internal bone level (IB). Right side shows half view of model without crown for clarity. Complete implant model and bone cylindrical part near the implant to evaluate bone strain more closely. B, Meshes of finite element model for 2 connection types.

MATERIAL AND METHODS

Twelve 3-dimensional (3D) finite element models were constructed (Fig. 1; Table 1). The models were designed based on 2 levels of bone density (low, high), 2 different connection types (internal tissue level [IT], internal bone level [IB]), and 3 implant diameters (3.5 mm, 4.0 mm, 4.5 mm). All the 3D models were constructed by using a modeling software program (3-matic Research 9.0; Materialise Corp). Each model consisted of a mandibular bone section of the molar region with a nerve canal and implant complex (Fig. 1). Bone tissue was modeled with cancellous bone in the center, surrounded by a 2-mm layer of cortical bone.[17] Two levels of cancellous bone density (low, high) were considered to evaluate the effect of different bone densities on these systems. A cylindrical part near the bone-implant interface (0.33 mm from the implant thread and 0.55 mm from the bottom of the implant) was also set to thoroughly investigate the surrounding area of the implant (Fig. 1). The cylindrical part was a virtual window for measurement, not a physical

Table 1. Model description

Cancellous Bone Density	Connection Type	Diameter (mm)
Low	IT	3.5
		4.0
		4.5
	IB	3.5
		4.0
		4.5
High	IT	3.5
		4.0
		4.5
	IB	3.5
		4.0
		4.5

IB, internal bone level; IT, internal tissue level.

Table 2. Mechanical properties of materials used in finite element models

Material	Young Modulus (MPa)	Poisson Ratio	Reference
Crown	140000	0.28	Rungsiyakull et al[33]
Titanium	110000	0.34	Bulaqi et al[6]
Cement	10 760	0.35	Tolidis et al[34]
Cortical bone	13 700	0.30	Barbier et al[35]
Cancellous bone	–	–	–
Low density	259	0.30	Sugiura et al[36]
High density	3507	0.30	Sugiura et al[36]
Nerve canal	70	0.45	Vaillancourt et al[37]

Table 3. Number of tetrahedral elements and nodes for each part in models of 6 implant systems

Model	IT3510	IT4010	IT4510	IB3510	IB4010	IB4510
Element	1 300 548	1 390 543	1 443 195	1 421 108	1 640 428	1 661 340
Node	251 659	268 476	278 377	267 357	312 300	316 262

IT3510, model of IT with 3.5-mm diameter and 10-mm length; IT4010, model of IT with 4-mm diameter and 10-mm length; IT4510, model of IT with 4.5-mm diameter and 10-mm length; IB3510, model of IB with 3.5-mm diameter and 10-mm length; IB4010, model of IB with 4-mm diameter and 10-mm length; IB4510, model of IB with 4.5-mm diameter and 10-mm length.

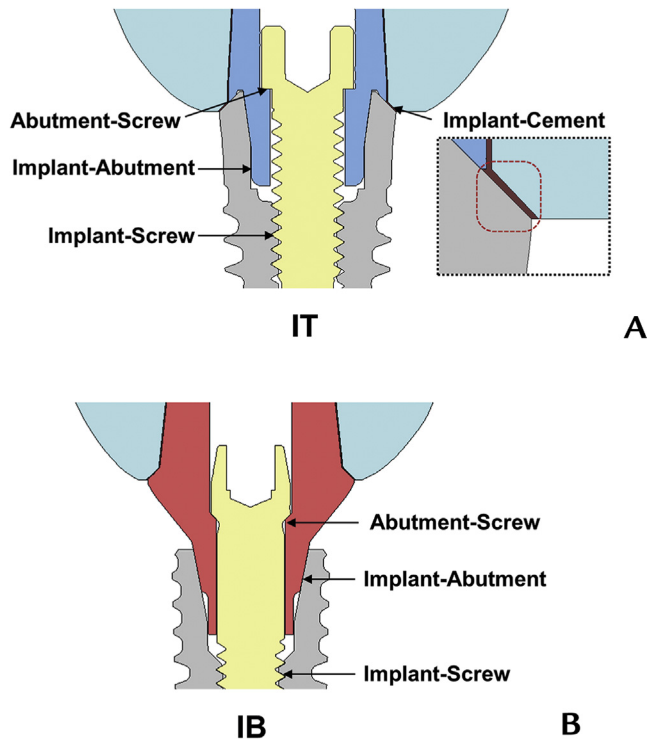

Figure 2. Interface conditions used in 2 types of implant system. A, Internal tissue level (IT). B, Internal bone level (IB).

part; therefore, the same material properties are also used in this part. The implant complex included the crown, cement layer, abutment, screw, and implant. All implants in the study were 10 mm in length and had 3 possible diameters (3.5 mm, 4.0 mm, and 4.5 mm). The design of the implant complex was provided by the manufacturer (Osstem Implant).

The material properties were determined based on previous literature (Fig. 1; Table 2).[6,33-37] All materials were assumed to be linearly elastic, homogenous, and isotropic. Table 3 lists the total number of elements for each model. To simulate complete osseointegration, the implant-bone interface was defined as a tie. The implant-abutment, abutment-screw, and abutment-cement layer contacts were assumed as contacts, and all other contacts were assumed as a tie (Fig. 2). Friction coefficients of 0.16, 0.441, and 0.25 were used for the implant-abutment, abutment-screw, and abutment-cement layer interfaces, respectively.[38,39] The boundary conditions were established as fixed in all axes (x, y, z) at the mesial and distal surfaces of the cortical and cancellous bone.[40]

The simulation was performed in 2 steps. In the first step, to simulate a tightening torque of 32 Ncm, the preload as calculated using the formula established by Bickford[41] was applied to the screw.[39,42] In the second step, the external force was applied to the crown to simulate masticatory loading. Two loading conditions were considered. A total force of 200 N was applied to 60 nodes on 3 cusps and 3 fosse in the vertical direction and of 100 N to 30 nodes on 3 cusps in the oblique direction (Fig. 3).[43,44]

All finite element analyses were performed by using a finite element analysis software program (ABAQUS 6.14; Dassault Systèmes SIMULIA Corp). The von Mises stress values were used to evaluate the stress distribution in the implant and abutment. The maximum and minimum principal strain were evaluated for bone tissue. The cylindrical part of the bone surrounding the dental implant was used to evaluate the 4 strain levels: atrophy (<200 με), maintenance (200 to 2500 με), hypertrophy (2500 to 4000 με), and fatigue failure (>4000 με) established by the Frost mechanostat theory.[45] To measure the tissue volume with a strain level, the volumes of each finite element with the corresponding elemental strain level were used.

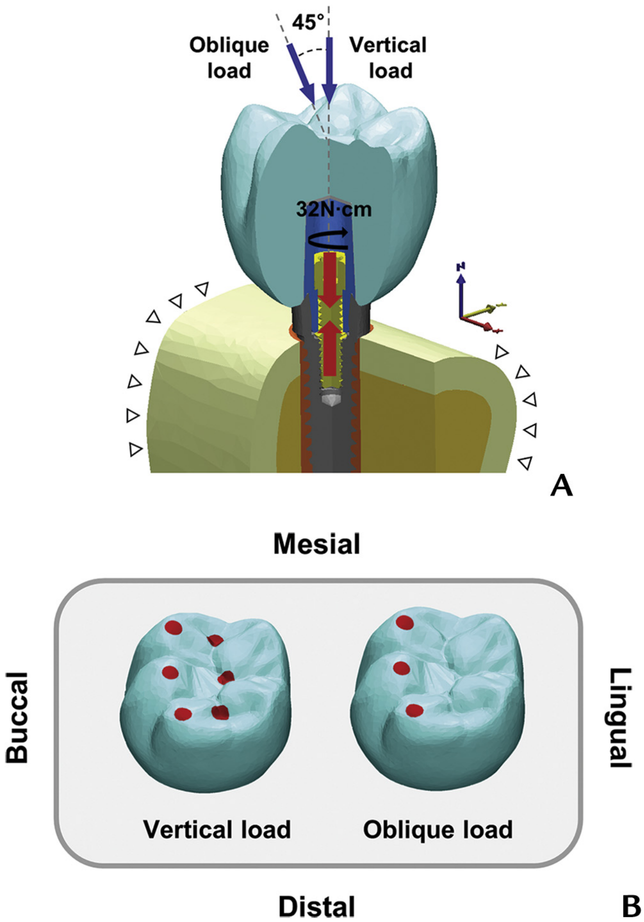

Figure 3. A, Loading and boundary conditions: hollow triangle represents boundary condition, *red* arrows illustrate preload on screw to achieve tightening torque of 32 Ncm, and *blue* arrows show 2 types of occlusal force. B, Each occlusion area according to loading type (vertical load, oblique load).

Each case was simulated once, and the maximum values of the von Mises stress and microstrain of 50 elements were collected: each finite element had 1 elemental stress and strain value, and those were treated as independent measures, as each element had a unique response because of its 3D size, shape, and position.[46] The maximum 50 values of the elemental von Mises stress and principal strain were considered as representative values in each case. For statistical analysis, the effects of 4 different factors were assessed by using the general linear model univariate procedure in a statistical software program (IBM SPSS Statistics, v20.0; IBM Corp).[47] Twenty-four sets were created to consider the effect of 2 levels of bone density, 2 connection types, 2 types of loading condition, and 3 implant diameters. The analysis of the main effects, 2-way, 3-way, and 4-way interactions were performed as per the literature (α=.05).[47-50] Partial eta squared (η_P^2) analyses were

Table 4. Maximum and minimum principal strain and von Mises stress

Results	Average	SD	Lowest	Largest
Maximum principal strain (με)				
Cortical bone	3 103.6	1 512.3	698.0	7 952.5
Cancellous bone	4 630.3	3 761.2	697.0	13 637.5
Minimum principal strain (με)				13 637.5
Cortical bone	-7 253.2	4 100.4	-1 950.0	-19 542.1
Cancellous bone	-4 133.2	2 739.2	-786.0	-10 068.5
von Mises stress (MPa)				
Implant	364.3	208.8	136.0	825.0
Abutment	402.7	269.6	121.5	946.5

performed to investigate the effect size of each factor.[48-50] The Tukey honestly significant difference test was used as a post hoc test for differences among 3 levels of implant diameter to assess interactions among the groups. The mean, standard deviation, lowest values, and highest values were calculated.[47]

RESULTS

The mean, lowest value, highest value, and standard deviation of maximum principal strain, minimum principal strain, and von Mises stress for independent factors are summarized in Tables 4 and 5. The effects of the independent factors on stress and strain distribution are summarized in Tables 6 and 7 and in Figure 4.

The highest maximum principal strain was observed in the IB with 4-mm diameter in low-density cortical bone under oblique loading. The highest value (in magnitude) of minimum principal strain was observed in IB with 3.5-mm diameter in low-density cortical bone under oblique loading. The loading type showed the highest influence on cortical bone (η_P^2=0.908). The highest value of maximum strain was observed in the IT with 4-mm diameter in low-density cancellous bone under oblique loading, whereas the minimum principal strain was observed in the IB in the same situation. The bone density indicated a significant effect on cancellous bone (η_P^2=0.982)

Figure 5 illustrates the microstrain distribution of bone tissue at low density. The strains were concentrated in a lingual direction at the bone tissue near the implant. In all models, the largest strain value (in magnitude) under oblique loading was higher than that under vertical loading. Low-density bone induced a larger maximum strain value (in magnitude) than high-density bone in both maximum and minimum principal strains (*P*<.001).

In the cortical bone, the IB under oblique loading showed larger maximum values in the minimum principal strains (in magnitude) as compared with the IT (*P*<.001). There were significant differences (*P*<.001) in minimum principal strain values for implant diameter, whereas the 3.5-mm diameter and 4-mm diameter

Table 5. Results of microstrain and von Mises stress for different 4 factors

	Cortical Bone				Cancellous Bone			
Factors	**Average**	**SD**	**Lowest**	**Largest**	**Average**	**SD**	**Lowest**	**Largest**
Maximum principal strain (με)								
Bone density								
Low	3516.5	1224.8	2003.4	7952.5	8004.4	2304.5	4563.9	13 637.5
high	2690.7	1654.1	698.0	6770.2	1256.2	446.6	697.0	2229.7
Connection type								
IT	2915.9	1467.7	698.0	6724.5	5019.6	4130.9	697.0	13 637.5
IB	3291.3	1533.9	996.4	7952.5	4241.0	3309.0	748.7	11 941.7
Loading								
vertical	1819.7	737.2	698.0	3686.8	3412.8	2644.8	697.0	8090.0
Oblique	4387.5	855.4	2789.7	7952.5	5847.9	4284.0	1378.7	13 637.5
Diameter								
3.5 mm	3331.3	1579.5	880.9	6724.5	4406.7	3499.0	748.7	12 672.4
4.0 mm	3309.6	1648.6	754.1	7952.5	4775.0	3957.2	767.8	13 637.5
4.5 mm	2669.9	1173.4	698.0	4768.3	4709.3	3812.1	697.0	12 794.9
Minimum principal strain (με)								
Bone density								
Low	-7832.9	3949.9	-3320.0	-19 542.1	-6746.0	959.6	-4757.6	-10 068.5
High	-6673.6	4168.8	-1950.0	-18 752.9	-1520.4	648.9	-786.0	-3126.8
Connection type								
IT	-5243.3	2157.3	-1950.0	-11 688.7	-4346.1	2843.0	-786.0	-9544.1
IB	-9263.1	4572.4	-3082.8	-19 542.1	-3920.3	2616.3	-787.3	-10 068.5
Loading								
Vertical	-4253.3	1348.1	-1950.0	-9624.8	-3555.7	2680.4	-786.0	-8644.9
Oblique	-10 253.1	3715.9	-4833.6	-19 542.1	-4710.7	2676.9	-1509.7	-10 068.5
Diameter								
3.5 mm	-8054.1	4453.0	-2524.9	-18 938.2	-4149.5	2609.4	-848.6	-8644.9
4.0 mm	-7613.9	4256.3	-2297.0	-19 542.1	-4342.9	2987.1	-867.4	-10 068.5
4.5 mm	-6091.6	3233.0	-1950.0	-13 876.3	-3907.2	2592.2	-786.0	-8153.6
	Implant				Abutment			
	Average	SD	Lowest	Largest	Average	SD	Lowest	Largest
von Mises stress (MPa)								
Bone density								
Low	366.0	208.1	136.2	822.4	416.5	282.5	123.9	946.5
high	362.6	209.8	136.0	825.1	388.9	255.7	121.5	879.0
Connection type								
IT	232.7	77.0	136.0	472.6	213.8	71.9	121.5	329.2
IB	495.9	216.1	220.6	825.0	591.6	262.5	193.7	946.5
Loading								
Vertical	226.7	67.6	136.0	422.1	262.6	193.1	121.5	877.9
Oblique	501.9	211.7	225.7	825.0	542.9	262.5	260.1	946.5
Diameter								
3.5 mm	399.5	231.3	136.0	825.0	483.1	291.7	121.5	946.5
4.0 mm	364.6	203.1	157.6	791.1	361.5	267.7	132.7	908.7
4.5 mm	328.8	183.9	310.8	346.9	363.6	228.1	144.2	807.5

IB, internal bone level; IT, internal tissue level; SD, standard deviations.

presented similar strain values of maximum principal strain (P>.05).

In the cancellous bone, the influence of diameter on the maximum principal strain of the bone varied based on implant design and loading condition, whereas for the minimum principal strain, a decrease in diameter increased the maximum value in terms of magnitude (P<.001), except for the IB model under oblique loading. For maximum principal strain, the implant with a 3.5-mm diameter represented a higher strain value than implants with 4-mm and 4.5-mm diameters (P<.001).

Figures 6 and 7 show the bone volume in the ranges of atrophy (<200 με), maintenance (200 to 2500 με), hypertrophy (2500 to 4000 με), and fatigue failure (>4000

Table 6. Specific results to verify influence of 4 factors

	Maximum Principal Strain		Minimum Principal Strain		von Mises Stress	
Source	**Cortical Bone**	**Cancellous Bone**	**Cortical Bone**	**Cancellous Bone**	**Implant**	**Abutment**
Density	<.001	<.001	<.001	<.001	<.05	<.001
Connection	<.001	<.001	<.001	<.001	<.001	<.001
Loading	<.001	<.001	<.001	<.001	<.001	<.001
Diameter	<.001	<.001	<.001	<.001	<.001	<.001
Density×connection	<.001	<.001	0.18	<.001	<.001	<.001
Connection×diameter	<.001	<.001	<.001	<.001	<.001	<.001
Connection×loading	<.05	<.001	<.001	0.46	<.001	<.001
Density×diameter	<.001	<.001	<.001	<.001	0.93	<.001
Density×loading	<.001	<.001	<.001	1.00	<.001	<.001
Loading×diameter	<.001	<.001	<.001	0.13	<.001	<.001
Density×connection×diameter	<.001	<.001	<.05	<.001	<.001	<.001
Density×connection×loading	<.05	<.001	0.35	<.001	<.05	<.001
Connection×loading×diameter	<.001	<.05	<.001	<.001	<.001	<.001
Density×loading×diameter	0.98	<.001	0.37	<.001	<.001	<.001
Density×connection×loading×diameter	0.08	<.001	0.159	<.05	0.901	<.001

Table 7. Effect size regarding 4 factors

	Maximum Principal Strain		Minimum Principal Strain		von Mises Stress	
Source	**Cortical Bone**	**Cancellous Bone**	**Cortical Bone**	**Cancellous Bone**	**Implant**	**Abutment**
Density	0.504	0.982	0.270	0.982	0.004	0.195
Connection	0.173	0.415	0.816	0.264	0.962	0.978
Loading	0.907	0.874	0.908	0.725	0.965	0.962
Diameter	0.359	0.108	0.438	0.201	0.550	0.805
Density×connection	0.010	0.417	–	0.114	0.041	0.177
Connection×diameter	0.161	0.020	0.131	0.054	0.181	0.813
Connection×loading	0.008	0.058	0.604	–	0.883	0.861
Density×diameter	0.023	0.129	0.020	0.214	–	0.232
Density×loading	0.282	0.747	0.028	–	0.029	0.065
Loading×diameter	0.185	0.025	0.184	–	0.375	0.682
Density×connection×diameter	0.019	0.057	0.010	0.202	0.021	0.231
Density×connection×loading	0.006	0.047	–	0.038	0.006	0.056
Connection×loading×diameter	0.107	0.009	0.022	0.191	0.079	0.741
Density×loading×diameter	–	0.048	–	0.053	0.022	0.095
Density×connection×loading×diameter	–	0.017	–	0.007	–	0.095

με). For cancellous bone, a low bone density induced a large (up to 22%) bone volume in the range of hypertrophy and fatigue failure, whereas high bone density resulted in almost no bone volume in the hypertrophy or fatigue failure regions. However, high bone density induced large (up to 64%) bone volume in the atrophy range (P<.001). For cortical bone, although the sum of the bone volume in the hypertrophy and fatigue failure regions for IB was still small (up to 12%), the IB for high bone density induced greater bone volume in minimum principal strain for the fatigue failure regions as compared with the IT (P<.001).

Figure 8 illustrates the von Mises stress distribution of the implant complexes under oblique loading. In both implant and abutment, the stress values were highest in IB with 3.5-mm diameters under oblique loading.

For the implant, the largest von Mises stress values were observed in IB with 3.5-mm diameters in high-density bone under oblique loading. In all cases, the implants with 3.5-mm diameters presented the maximum stress values (P<.001). High concentrations were observed in the lingual area of the implant collar. As the diameter of the implant increased, the maximum von Mises stress also increased (P<.001).

For the abutment, low-density bone induced a higher stress value than did high-density bone. In all models, the magnitude of the stress value in the abutment was influenced by the implant diameter (P<.001): decreasing

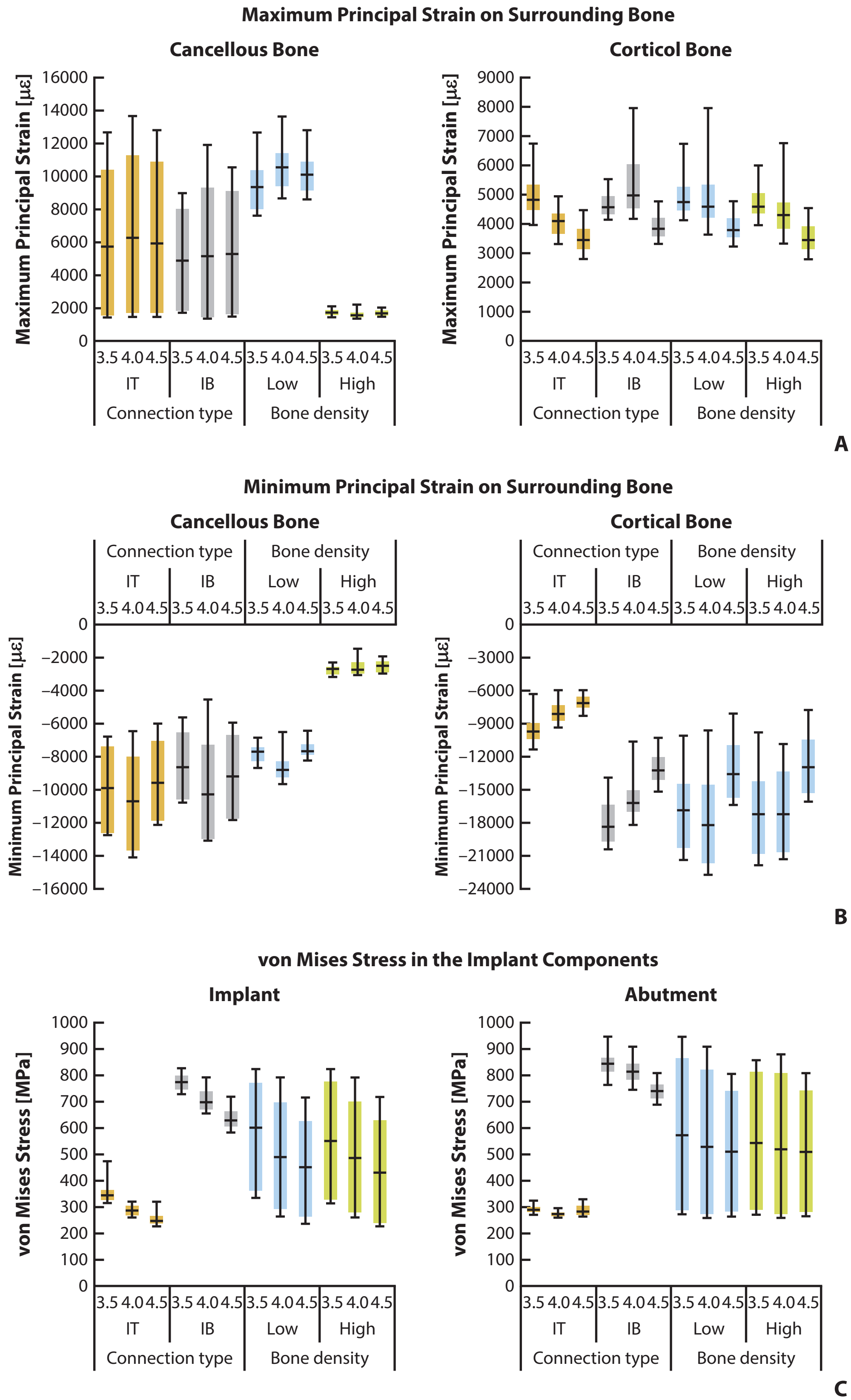

Figure 4. Main results under oblique load considering 3 study factors (connection type, low and high bone density, implant diameter). A, Maximum principal strain on cancellous bone and cortical bone. B, Minimum principal strain on cancellous bone and cortical bone. C, von Mises stress on implant and abutment. IT, internal tissue level; IB, internal bone level.

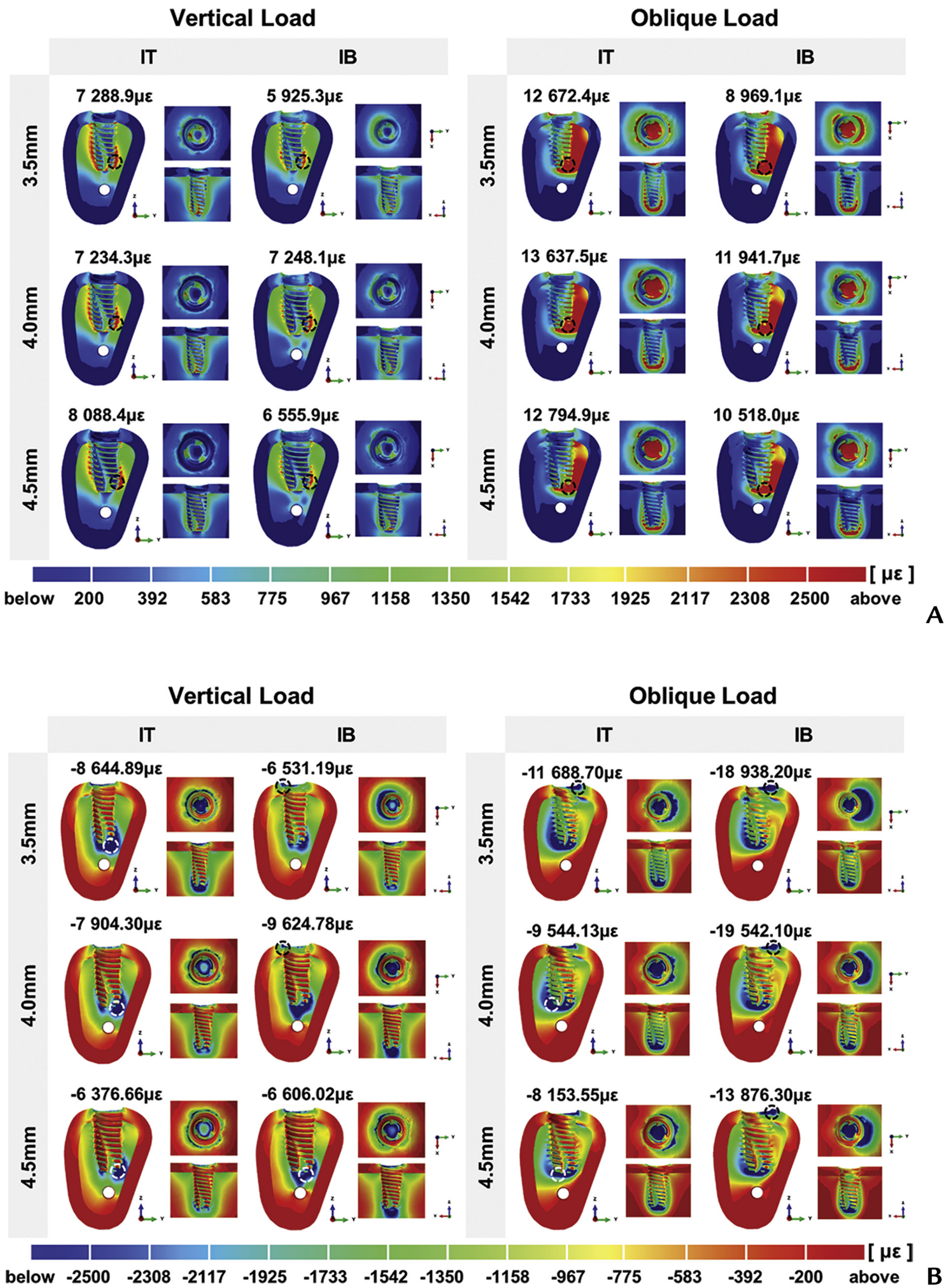

Figure 5. Bone strain distribution for low-density bone and position and largest strain value (in magnitude) presented for each section. A, Maximum principal strain. B, Minimum principal strain. IT, internal tissue level; IB, internal bone level.

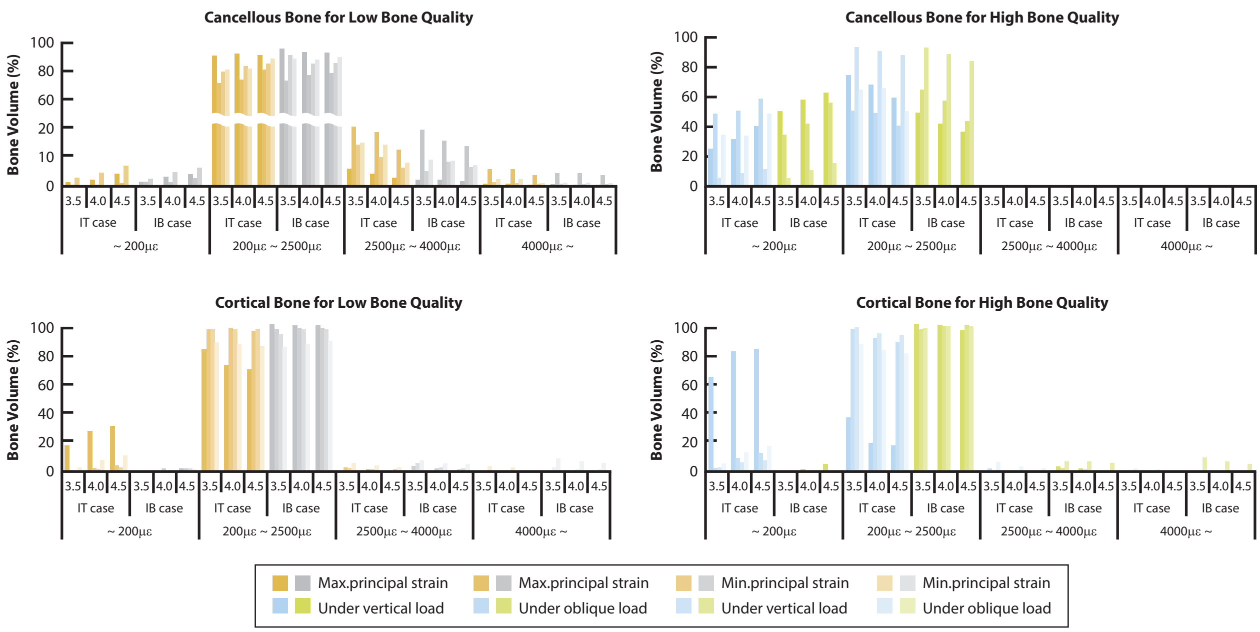

Figure 6. Strain distribution of surrounding bone as per 4 strain level ranges: cancellous bone for low bone quality, cancellous bone for high bone quality, cortical bone for low bone quality, and cortical bone for high bone quality. IT, internal tissue level; IB, internal bone level.

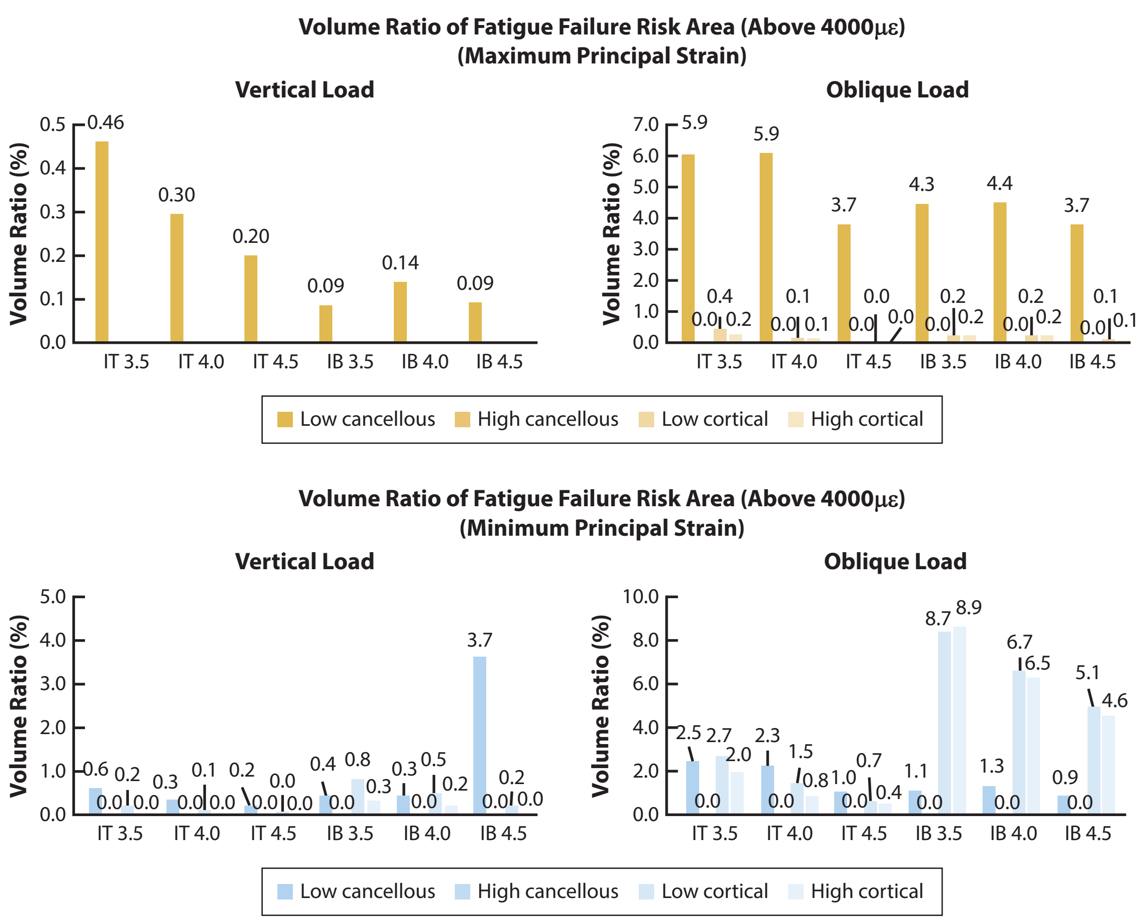

Figure 7. Specific bone volume ratio in fatigue failure region; maximum principal strain distribution under vertical load, maximum principal strain distribution under oblique load, minimum principal strain distribution under vertical load, and minimum principal strain distribution under oblique load. IT, internal tissue level; IB, internal bone level.

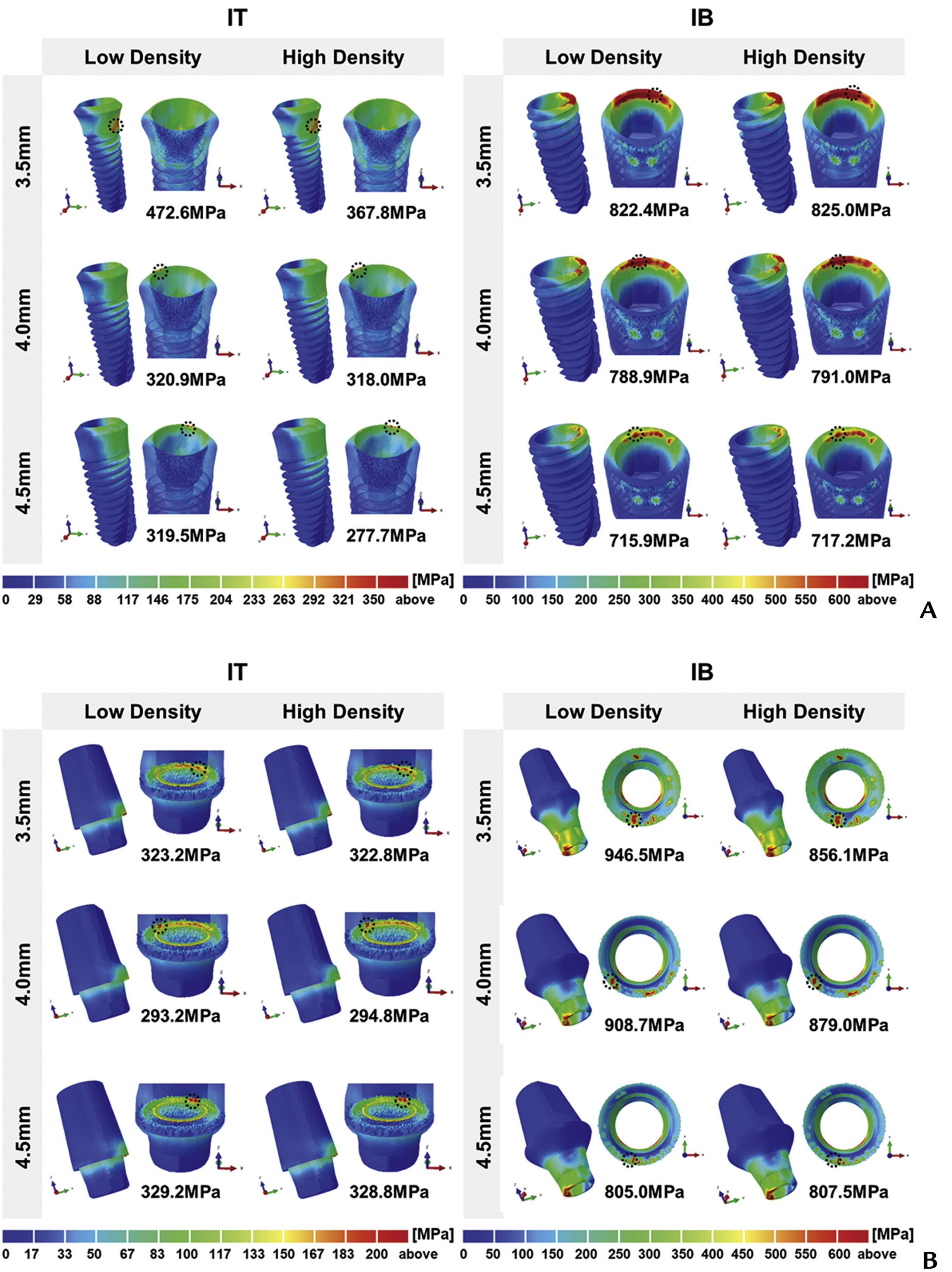

Figure 8. Stress distribution in implant components under oblique load. A, Implant. B, Abutment. IT, internal tissue level; IB, internal bone level.

the implant diameter increased the stress concentration. The largest stress values in the IB were found at the seat of the abutment screw.

DISCUSSION

The present study revealed that implant diameter, implant-abutment connection type, bone density, and loading condition influenced the biomechanical behavior in terms of stress distributions in both implant and abutment and of bone strain distributions. Thus, the null hypothesis that different prosthesis features would not result in different stress or strain values in implant components and surrounding bones was rejected.

The differences in strain and stress distribution were evaluated for tissue-level and bone-level implants. The connection type demonstrated a higher influence on the stress value (implant: η_P^2=0.962; abutment: η_P^2=0.978) than other factors, whereas bone density showed the lowest influence (implant: η_P^2=0.004; abutment: η_P^2=0.195). The IB group would induce a significantly higher stress value than the IT group. The average stress of the implants and abutments in the IB group were 2 to 3 times higher than that of the IT group. This result conflicts with a similar previous study by Chang et al,[51] who reported that the stress of the bone-level implant was less than that of the tissue-level implant. The size of the abutment was also smaller than that used in the present study, which would also decrease the thickness of the abutment. In the IT group, the maximum stress value was about half the yield strength of titanium grade 5 at a 3.5-mm diameter and under oblique loading conditions; in the IB group under these same conditions, this value was close to the yield strength.[52]

As per the results of the present study, the main effect and the interaction effects of the 4 variables were significant on the implant stress value ($P<.05$), except for the combination of bone density and implant diameter ($P>.05$). Overall, the stress value of the IT group was less than 50% of the yield strength in all conditions. In the IB group, the stress of the implant was highly concentrated on the margin of the connection, which was close to the yield strength. As the diameter increased from 3.5 mm to 4.5 mm, the stress level decreased to about 15% in the implant and abutment. Little difference was noted in the stress of the implant and abutment based on bone density. The difference in bone density of the cancellous bone did not affect the implant stress, whereas the difference in implant diameter did. In general, the results of present study indicated that the IT was more biomechanically stable than the IB. The placement of a 3.5-mm IB implant in the posterior region seems not to be the appropriate choice when normal or increased occlusal force is applied.[53,54] The difference in connection had a greater effect on the stress than the difference in diameter did.

Regarding the minimum principal strain related to the compressive stress on the surrounding bone, the value of the IB was twice than that of the IT on the cortical bone. The strain value of the cancellous bone was primarily affected by bone density (η_P^2=0.982), and loading condition has a major influence on cortical bone (η_P^2=0.908). For cancellous bone, no significant effect of binary combinations was found between the loading condition and another factor ($P>.05$); the strain values under oblique loading were higher than those under vertical loading in all combinations. The effects of the ternary and quaternary combinations of 4 independent factors were significant for all combinations ($P<.05$). Bone fracturing can occur if the strain value is about 25 000 με or greater.[22] A maximum strain value of about 19 000 με was observed at diameters of 3.5 and 4.0 mm in the IB group, which, in spite of being quite high, is still lower than the fracture limit. In the model of low-density cancellous bone, the IT appeared to be better than the IB when a 3.5-mm diameter implant was selected for a narrow posterior alveolar ridge.

Calculating not only the peak of the strain but also the volume of the fatigue failure risk area surrounding the implants using finite element analysis was assumed to be important. The maximum and minimum principal strain are related to tensile and compressive stress, respectively, and bone is more resistant to fracture under compressive rather than tensile strain.[55] The volume ratio of compressive strain within the fatigue failure risk region was focused on the cortical bone, whereas the volume ratio of tensile strain was relatively more concentrated on the cancellous bone under oblique loading conditions. How much the area within the fatigue failure risk region would be affected in actual clinical conditions is unclear because occlusal force is applied for approximately only 8 minutes per day.[56]

Limitations of the present study included that certain aspects such as 3D modeling, preload, contact, and loading condition were considered in detail to obtain results closer to reality. However, the stress concentration of the abutment and implant would be different from the clinical situation because of the small nonlinear deformation when stress is greater than the yield strength. Although cone beam computed tomography has been widely using for implant surgery, it may not be accurate enough to use cone beam computed tomography gray density values to determine the bone density because they are not absolute.[57,58] In addition, a simplified continuum shape and the material properties for the bone part were used in this study. Although bone is frequently modeled as a continuum structure in finite element studies, it is porous and encloses numerous large spaces, and low-density bone has more pores than high-density bone. In this study, only the Young modulus of the cancellous bone based on density was used to incorporate the different mechanical properties.[4,59,60] Thus, future studies using a more realistic bone model would be of value.

CONCLUSIONS

Based on the findings of this finite element analysis study, the following conclusions were drawn:

1. The tissue-level connection is more advantageous as compared with the bone-level connection in terms of stress distribution of the implant and abutment.
2. The selection of implant diameter and connection is important for stress distribution, and the type of connection has a greater impact on stress than the diameter does ($P<.001$).
3. Bone density was the most influential factor in the strain of both cancellous and cortical bone ($P<.001$).

REFERENCES

1. Weber H-P, Sukotjo C. Does the type of implant prosthesis affect outcomes in the partially edentulous patient? Int J Oral Maxillofac Implants 2007;22:140-72.
2. Schimmel M, Müller F, Suter V, Buser D. Implants for elderly patients. Periodontology 2000 2017;73:228-40.
3. Hartshorne J. Does bruxism contribute to dental implant failure. International Dentistry African Edition 2015;5:38-42.
4. Pjetursson BE, Thoma D, Jung R, Zwahlen M, Zembic A. A systematic review of the survival and complication rates of implant-supported fixed dental prostheses (FDP s) after a mean observation period of at least 5 years. Clin Oral Implants Res 2012;23:22-38.
5. Lobbezoo F, van der Zaag J, Naeije M. Bruxism: its multiple causes and its effects on dental implants–an updated review. J Oral Rehabil 2006;33:293-300.
6. Bulaqi HA, Mashhadi MM, Safari H, Samandari MM, Geramipanah F. Effect of increased crown height on stress distribution in short dental implant components and their surrounding bone: A finite element analysis. J Prosthet Dent 2015;113:548-57.
7. Oftadeh R, Perez-Viloria M, Villa-Camacho JC, Vaziri A, Nazarian A. Biomechanics and mechanobiology of trabecular bone: a review. J Biomech Eng 2015;137:0108021-01080215.
8. Lee H, Park S, Noh G. Biomechanical analysis of 4 types of short dental implants in a resorbed mandible. J Prosthet Dent 2019;121:659-70.
9. Lee H, Park S, Kwon K-R, Noh G. Effects of cementless fixation of implant prosthesis: A finite element study. J Adv Prosthodont 2019;11:341-9.
10. Park S-M, Park S, Shin S, Lee H, Ahn S-J, Kim L, et al. Designing a mandibular advancement device with topology optimization for a partially edentulous patient. J Prosthet Dent 2020;123:850-9.
11. Lee H, Park S-M, Noh K, Ahn S-J, Shin S, Noh G. Biomechanical stability of internal bone-level implant: Dependency on hex or non-hex structure. Struct Eng Mech 2020;74:567-76.
12. Pellizzer EP, Verri FR, De Moraes SLD, Falcón-Antenucci RM, De Carvalho PSP, Noritomi PY. Influence of the implant diameter with different sizes of hexagon: analysis by 3-dimensional finite element method. Int J Oral Implantol 2013;39:425-31.
13. Moriwaki H, Yamaguchi S, Nakano T, Yamanishi Y, Imazato S, Yatani H. Influence of implant length and diameter, bicortical anchorage, and sinus augmentation on bone stress distribution: three-dimensional finite element analysis. Int J Oral Maxillofac Implants 2016;31:e84-91.
14. Tada S, Stegaroiu R, Kitamura E, Miyakawa O, Kusakari H. Influence of implant design and bone quality on stress/strain distribution in bone around implants: a 3-dimensional finite element analysis. Int J Oral Maxillofac Implants 2003;18:357-68.
15. Kondo T, Wakabayashi N. Influence of molar support loss on stress and strain in premolar periodontium: a patient-specific FEM study. J Dent 2009;37:541-8.
16. Wu T, Liao W, Dai N, Tang C. Design of a custom angled abutment for dental implants using computer-aided design and nonlinear finite element analysis. J Biomech 2010;43:1941-6.
17. Liu J, Pan S, Dong J, Mo Z, Fan Y, Feng H. Influence of implant number on the biomechanical behaviour of mandibular implant-retained/supported overdentures: a three-dimensional finite element analysis. J Dent 2013;41:241-9.
18. Tanasića I, Tihaček-Šojićb L, Milić-Lemićc A. Finite element analysis of compressive stress and strain of different implant forms during vertical loading. Int J Comput Dent 2014;17:125-33.
19. Marcián P, Borák L, Valášek J, Kaiser J, Florian Z, Wolff J. Finite element analysis of dental implant loading on atrophic and non-atrophic cancellous and cortical mandibular bone–a feasibility study. J Biomech 2014;47:3830-6.
20. Termeie D, Klokkevold PR, Caputo AA. Effect of implant diameter and ridge dimension on stress distribution in mandibular first molar sites—A photoelastic study. J Oral Implantol 2015;41:e165-73.
21. Yan X, Zhang X, Chi W, Ai H, Wu L. Comparing the influence of crestal cortical bone and sinus floor cortical bone in posterior maxilla bi-cortical dental implantation: a three-dimensional finite element analysis. Acta Odontol Scand 2015;73:312-20.
22. Frost HM. Bone "mass" and the "mechanostat": a proposal. Anat Rec 1987;219:1-9.
23. Tyrovola JB, Odont X. The "mechanostat theory" of frost and the OPG/Rankl/RANK system. J Cell Biochem 2015;116:2724-9.
24. Chou H-Y, Müftü S, Bozkaya D. Combined effects of implant insertion depth and alveolar bone quality on periimplant bone strain induced by a wide-diameter, short implant and a narrow-diameter, long implant. J Prosthet Dent 2010;104:293-300.
25. Sasada Y, Cochran DL. Implant-abutment connections: a review of biologic consequences and peri-implantitis implications. Int J Oral Maxillofac Implants 2017;32:1296-307.
26. Broggini N, McManus LM, Hermann J, Medina R, Oates T, Schenk R, et al. Persistent acute inflammation at the implant-abutment interface. J Dent Res 2003;82:232-7.
27. Al-Nsour MM, Chan H-L, Wang H-L. Effect of the platform-switching technique on preservation of peri-implant marginal bone: a systematic review. Int J Oral Maxillofac Implants 2012;27:138-45.
28. Sen N, Us YO. Fatigue survival and failure resistance of titanium versus zirconia implant abutments with various connection designs. J Prosthet Dent 2019;122:315.e1-7.
29. Camps-Font O, Martín-Fatás P, Clé-Ovejero A, Figueiredo R, Gay-Escoda C, Valmaseda-Castellón E. Postoperative infections after dental implant placement: Variables associated with increased risk of failure. J Periodontol 2018;89:1165-73.
30. Bordin D, Witek L, Fardin VP, Bonfante EA, Coelho PG. Fatigue failure of narrow implants with different implant-abutment connection designs. J Prosthodont 2018;27:659-64.
31. Wallner G, Rieder D, Wichmann MG, Heckmann SM. Peri-implant bone loss of tissue-level and bone-level implants in the esthetic zone with gingival biotype analysis. Int J Oral Maxillofac Implants 2018;33:1119-25.
32. Isler SC, Uraz A, Kaymaz O, Cetiner D. An Evaluation of the relationship between peri-implant soft tissue biotype and the severity of peri-implantitis: a cross-sectional study. Int J Oral Maxillofac Implant 2019;34:187-96.
33. Rungsiyakull C, Chen J, Rungsiyakull P, Li W, Swain M, Li Q. Bone's responses to different designs of implant-supported fixed partial dentures. Biomech Model Mechanobiol 2015;14:403-11.
34. Tolidis K, Papadogiannis D, Papadogiannis Y, Gerasimou P. Dynamic and static mechanical analysis of resin luting cements. J Mech Behav Biomed Mater 2012;6:1-8.
35. Barbier L, Sloten JV, Krzesinski G, Van Der Perre ES. Finite element analysis of non-axial versus axial loading of oral implants in the mandible of the dog. J Oral Rehabil 1998;25:847-58.
36. Sugiura T, Yamamoto K, Kawakami M, Horita S, Murakami K, Kirita T. Influence of bone parameters on peri-implant bone strain distribution in the posterior mandible. Med Oral Patol Oral Cir Bucal 2015;20:66-73.
37. Vaillancourt H, Pilliar R, McCammond D. Finite element analysis of crestal bone loss around porous-coated dental implants. J Appl Biomater 1995;6:267-82.
38. Guda T, Ross TA, Lang LA, Millwater HR. Probabilistic analysis of preload in the abutment screw of a dental implant complex. J Prosthet Dent 2008;100:183-93.
39. Wang R-F, Kang B, Lang LA, Razzoog ME. The dynamic natures of implant loading. J Prosthet Dent 2009;101:359-71.
40. Huang H-L, Hsu J-T, Fuh L-J, Tu M-G, Ko C-C, Shen Y-W. Bone stress and interfacial sliding analysis of implant designs on an immediately loaded maxillary implant: a non-linear finite element study. J Dent 2008;36:409-17.
41. Bickford J. An introduction to the design and behavior of bolted joints, Revised and expanded. 3rd ed. New York: CRC press; 1995. p. 894.
42. Lang LA, Kang B, Wang R-F, Lang BR. Finite element analysis to determine implant preload. J Prosthet Dent 2003;90:539-46.
43. Chen J, Zhang Z, Chen X, Zhang X. Influence of custom-made implant designs on the biomechanical performance for the case of immediate post-extraction placement in the maxillary esthetic zone: a finite element analysis. Comput Methods Biomech Biomed Engin 2017;20:636-44.
44. Torcato LB, Pellizzer EP, Verri FR, Falcón-Antenucci RM, Júnior JFS, de Faria Almeida DA. Influence of parafunctional loading and prosthetic connection

on stress distribution: A 3D finite element analysis. J Prosthet Dent 2015;114:644-51.
45. Roberts WE, Huja S, Roberts JA. Bone modeling: biomechanics, molecular mechanisms, and clinical perspectives. Semin Orthod 2004;10:123-61.
46. Minatel L, Verri FR, Kudo GAH, de Faria Almeida DA, de Souza Batista VE, Lemos CAA, et al. Effect of different types of prosthetic platforms on stress-distribution in dental implant-supported prostheses. Mater Sci Eng C 2017;71:35-42.
47. Rekow ED, Harsono M, Janal M, Thompson VP, Zhang G. Factorial analysis of variables influencing stress in all-ceramic crowns. Dent Mater 2006;22:125-32.
48. Lümkemann N, Eichberger M, Stawarczyk B. Bond strength between a high-performance thermoplastic and a veneering resin. J Prosthet Dent 2020;124:790-7.
49. Kim H-K, Kim S-H, Lee J-B, Ha S-R. Effects of surface treatments on the translucency, opalescence, and surface texture of dental monolithic zirconia ceramics. J Prosthet Dent 2016;115:773-9.
50. Ilie N, Stawarczyk B. Quantification of the amount of blue light passing through monolithic zirconia with respect to thickness and polymerization conditions. J Prosthet Dent 2015;113:114-21.
51. Chang H-S, Chen Y-C, Hsieh Y-D, Hsu M-L. Stress distribution of two commercial dental implant systems: A three-dimensional finite element analysis. J Dent Sci 2013;8:261-71.
52. Boyer R, Collings EW, Welsch G. Materials properties handbook: Titanium Alloys. Materials Park, OH: ASM International; 1994:312.
53. Koc D, Dogan A, Bek B. Bite force and influential factors on bite force measurements: a literature review. Eur J Dent 2010;4:223-32.
54. AL-Omiri MK, Sghaireen MG, Alhijawi MM, Alzoubi IA, Lynch CD, Lynch E. Maximum bite force following unilateral implant-supported prosthetic treatment: within-subject comparison to opposite dentate side. J Oral Rehabil 2014;41:624-9.
55. Keaveny TM, Wachtel EF, Ford CM, Hayes WC. Differences between the tensile and compressive strengths of bovine tibial trabecular bone depend on modulus. J Biomech 1994;27:1137-46.
56. Kato T, Thie NM, Huynh N, Miyawaki S, Lavigne GJ. Topical review: sleep bruxism and the role of peripheral sensory influences. J Orofac Pain 2003;17:191-213.
57. Pauwels R, Jacobs R, Singer SR, Mupparapu M. CBCT-based bone quality assessment: are Hounsfield units applicable? Dentomaxillofac Radiol 2015;44:1-16.
58. Cassetta M, Stefanelli LV, Pacifici A, Pacifici L, Barbato E. How accurate Is CBCT in measuring bone density? A comparative CBCT-CT in vitro study. Clin Implant Dent Relat Res 2014;16:471-8.
59. Keyak JH, Rossi SA, Jones KA, Skinner HB. Prediction of femoral fracture load using automated finite element modeling. J Biomech 1997;31:125-33.
60. Keyak J, Lee I, Skinner H. Correlations between orthogonal mechanical properties and density of trabecular bone: use of different densitometric measures. J Biomed Mater Res 1994;28:1329-36.

Corresponding author:
Dr Gunwoo Noh
School of Mechanical Engineering
Korea University
Anam-dong, Seongbuk-gu, Seoul, 136-713
REPUBLIC OF KOREA
Email: gunwoonoh@korea.ac.kr

Acknowledgments
The authors thank the Osstem Implant for supporting the STL files of implants and abutments which helped to perform this research.

https://doi.org/10.1016/j.prosdent.2020.08.042